Archives of Biochemistry and Biophysics 606 (2016) 180–188

Contents lists available at ScienceDirect

Archives of Biochemistry and Biophysics

journal homepage: www.elsevier.com/locate/yabbi

Identification of structural determinants of NAD(P)H selectivity and lysine binding in lysine N^6-monooxygenase

Heba Abdelwahab [a, b], Reeder Robinson [a, 1], Pedro Rodriguez [a], Camelia Adly [b], Sohby El-Sohaimy [c], Pablo Sobrado [a, d, e, *]

[a] Department of Biochemistry, Virginia Tech, Blacksburg, VA 24061, USA
[b] Department of Chemistry, Faculty of Science, Damietta University, Damietta, 34517, Egypt
[c] Department of Food Technology, Arid Lands Cultivation Research Institute, City of Scientific Research and Technological Applications, Alexandria, 21934, Egypt
[d] Fralin Life Science Institute, Virginia Tech, Blacksburg, VA 24061, USA
[e] Virginia Tech Center for Drug Discovery, Virginia Tech, Blacksburg, VA 24061, USA

ARTICLE INFO

Article history:
Received 27 June 2016
Received in revised form
22 July 2016
Accepted 1 August 2016
Available online 5 August 2016

Keywords:
Flavin-dependent monooxygenases
N-hydroxylating monooxygenases
L-lysine hydroxylase
Nocobactin
Siderophores
Virulence factor
C4a-hydroperoxyflavin

ABSTRACT

L-lysine (L-Lys) N^6-monooxygenase (NbtG), from *Nocardia farcinica*, is a flavin-dependent enzyme that catalyzes the hydroxylation of L-Lys in the presence of oxygen and NAD(P)H in the biosynthetic pathway of the siderophore nocobactin. NbtG displays only a 3-fold preference for NADPH over NADH, different from well-characterized related enzymes, which are highly selective for NADPH. The structure of NbtG with bound $NAD(P)^+$ or L-Lys is currently not available. Herein, we present a mutagenesis study targeting M239, R301, and E216. These amino acids are conserved and located in either the NAD(P)H binding domain or the L-Lys binding pocket. M239R resulted in high production of hydrogen peroxide and little hydroxylation with no change in coenzyme selectivity. R301A caused a 300-fold decrease on k_{cat}/K_m value with NADPH but no change with NADH. E216Q increased the K_m value for L-Lys by 30-fold with very little change on the k_{cat} value or in the binding of NAD(P)H. These results suggest that R301 plays a major role in NADPH selectivity by interacting with the 2′-phosphate of the adenine-ribose moiety of NADPH, while E216 plays a role in L-Lys binding.

1. Introduction

Nocardiosis is a localized or systemic infection that can occur in both immunocompromised and immunocompetent patients [1]. It is caused by aerobic, gram positive actinomycetes belonging to the genus *Nocardia* in the family *Nocardiaceae* [2]. *Nocardia cyriacigeorgica*, *Nocardia nova*, and *Nocardia farcinica* are the most common species that infect the respiratory system, producing acute or chronic pulmonary infections [3,4]. In addition, infections of the brain, central nervous system, heart, kidneys, lymph nodes, skin tissues, and bone marrow have also been reported [2,5]. The genome of *N. farcinica* IFM 10152 has recently been sequenced and annotated. This revealed the presence of a gene cluster that includes eight predicted genes (A, B, C, D, E, F, G, and H), and was shown to have similarity to the biosynthetic gene cluster of the siderophore mycobactin from *Mycobacterium tuberculosis* [6]. Based on sequence homology as well as gene organization, this gene cluster was proposed to be involved in the biosynthesis of the siderophore nocobactin in *N. farcinica* [7].

Siderophores are low molecular weight iron chelators that are synthesized and secreted by some microbial pathogen, including *Nocardia, Mycobacteria,* and other related species [8]. The ability of nocobactin to sequester iron influences the growth and virulence of *N. farcinica* [9]. The iron binding properties of siderophores depends on the chemical moieties that are able to coordinate iron, with the most common being catecholate, carboxylate, and hydroxamate [10]. Nocobactin biosynthetic pathway involves L-Lysine (L-Lys) hydroxylation by L-Lys ^{6}*N*-hydroxylase, also known as NbtG. Hydroxylated L-Lys is acylated and assembled into the nocobactin backbone by non-ribosomal peptide synthetases where it makes up the hydroxamate iron binding site [11].

NbtG is a member of the class B flavin monooxygenases, and is

* Corresponding author. Department of Biochemistry, Virginia Tech, Blacksburg, VA 24061, USA.
E-mail address: psobrado@vt.edu (P. Sobrado).
[1] Current address: Medical University of South Carolina, 70 President St, Charleston, SC 29425, United States.

http://dx.doi.org/10.1016/j.abb.2016.08.004
0003-9861/

grouped under the subfamily of *N*-hydroxylating monooxygenases (NMOs) [12]. The best characterized NMOs are the L-ornithine (L-Orn) monooxygenases from *Aspergillus fumigatus* (SidA) and *Pseudomonas aeruginosa* (PvdA) [13–18]. SidA displays an ~20-fold preference for NADPH over NADH, while PvdA is only able to react with NADPH [13,19,20]. Furthermore, SidA and PvdA form long-lived stable C4a-hydroperoxyflavin intermediates which are the key oxygenating species responsible for substrate hydroxylation [21]. The mechanism of stabilization has been studied in detail in SidA and involves interactions of C4a-hydroperoxyflavin with $NADP^+$, which remains bound throughout the catalytic cycle [15–18,22]. In contrast, NbtG does not form a stable C4a-hydroperoxyflavin species, resulting in low levels of L-Lys hydroxylation (~30%) and high levels of superoxide and hydrogen peroxide by-products. In addition, NbtG can utilize either NADH or NADPH with very similar affinities [12,23,24]. The lack of specificity of NbtG for NADPH was previously proposed to result from the absence of a conserved Arg residue equivalent to that found in SidA (R279), and PvdA (R240), which is capable of interacting with the 2′-phosphate of the adenine-ribose moiety in NADPH [15,16,18]. Using sequence alignment and structural superimposition, M239 was identified as being in the position of the Arg found in the L-Orn hydroxylases and was replaced with Arg. Further structural analyses also identified R301 as a residue in close proximity to the 2'-phosphate of NADPH (Figs. 1 and 2).

Another interesting feature of NMOs is the presence of the consensus sequence motif GGG(Q/N)S(G/A) within the NADPH binding domain [25]. Sequence alignment shows that the Q/N residue is not conserved in NbtG and that a glutamate (Glu216) is found instead. In PvdA and SidA, the Q/N residues (Gln217 and Gln256, respectively) have been proposed to be involved in NADP(H) binding; however, they have never been kinetically characterized [15,22,26]. In PvdA, Q217 is predicted to stabilize the loop conformation that exists between the first strand and the helix of the NADPH binding domain through hydrogen bonding with the

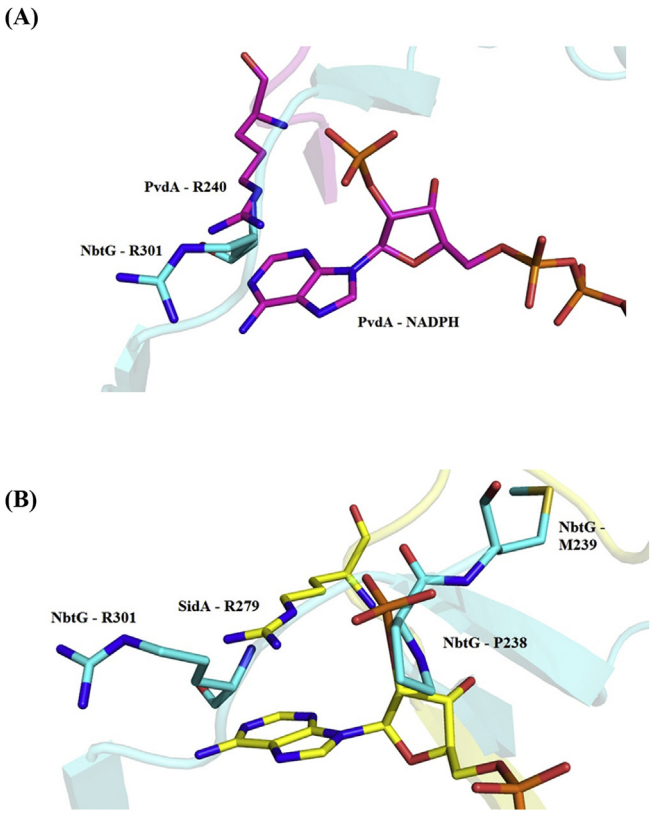

Fig. 2. Structure superimposition of (A) NbtG (PDB: 4D7E, cyan) on PvdA (PDB: 3S61, magenta) showing the functionally related Arg residue. (B) Structure superimposition of NbtG (cyan) on SidA (PDB: 4B63, yellow) showing the relative positions of the M239, P238, and R301 residues of NbtG (cyan) in comparison with R279 (yellow) in the SidA-NADPH bound structure. (For interpretation of the references to colour in this figure legend, the reader is referred to the web version of this article.)

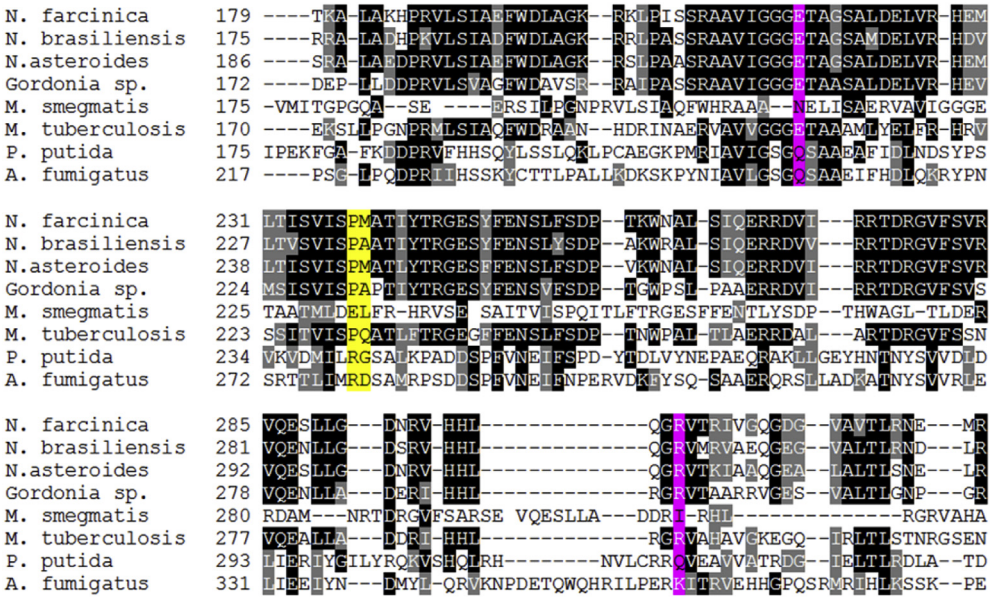

Fig. 1. Amino acid sequence alignment of NMOs. All the aligned enzymes are L-Lys monooxygenases except for the L-Orn monooxygenases from *P. putida* and *A. fumigatus*. Conserved amino acids targeted for site-directed mutagenesis (Magenta) are within the NADPH binding domain. R279 (SidA) and R240 (PvdA) indicated in yellow are aligned with P238 (NbtG). M239 is also highlighted in yellow. The alignment was created with T-coffee [46]. (For interpretation of the references to colour in this figure legend, the reader is referred to the web version of this article.)

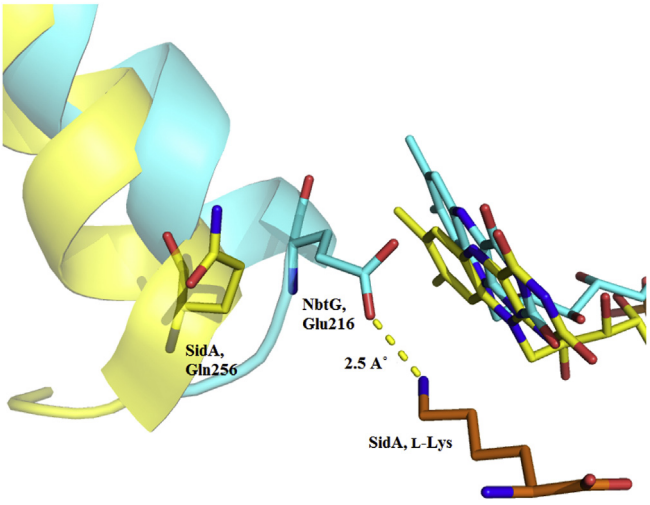

Fig. 3. Position of E216 residue in the NbtG (PDB: 4D7E, cyan). The structure was superimposed to the structure of SidA with L-Lys-bound SidA (PDB: 4B64; yellow). Lys (orange) is predicted to bind in NbtG in adjacent to the flavin m as observed in SidA. The potential hydrogen bond of E216 with L-Lys in NbtG is shown with dashed-yellow lines. (For interpretation of the references to colour in this figure legend, the reader is referred to the web version of this article.)

backbone nitrogen of Asp289. Gln256 in SidA forms an H-bond with $NADP^+$ in molecular dynamics simulations of the $NADP^+$-SidA complex [15,22,25]. In NbtG, the corresponding Glu216 residue is within H-bonding distance to the epsilon nitrogen of L-Lys (Fig. 3) [26]. Here, we probed the function of M239 and R301 and E216 by site-directed mutagenesis and biochemical characterization of M239R, R301A, and E216Q. The data are consistent with R301 and E216 playing important roles in NADPH selectivity and L-Lys binding, respectively.

2. Materials and methods

2.1. Materials

NADPH (purity ≥ 98%) was purchased from MP Biomedicals (Billerica, MA). NADH (purity ≥ 95%) and FAD (purity ≥ 95%) were purchased from Acros Organics (New Jersey, US) and Sigma (St. Louis, MO), respectively. Compound concentration was determined using the following absorption coefficients: NAD(P)H $\varepsilon_{340} = 6.22 \times 10^3\ M^{-1}\ cm^{-1}$, and FAD $\varepsilon_{450} = 11.3 \times 10^3\ M^{-1}\ cm^{-1}$. Buffers and media components were obtained from Fisher Scientific (Pittsburgh, PA). All solvents were reagent grade. DNA primers used for mutagenesis reactions were synthesized by Integrated DNA Technologies (Coralville, IA). Plasmid and gel purification kits were obtained from Qiagen (Valencia, CA). *Escherichia coli* BL21(DE3)-$T1^R$ and *E. coli* TOP10 chemically competent cells were from Fisher Scientific and Invitrogen (Carlsbad, CA), respectively. Chromatography columns were obtained from GE Healthcare.

2.2. Site-directed mutagenesis

All mutagenesis reactions were performed using the QuikChange (Agilent Technologies) method following manufacturer's instructions. Wild-type NbtG (wtNbtG) subcloned into pVP56K was used as the template [12]. The forward primer (5′ CGGTGGTGGT**CAG**ACCGCAGGTTCTGCAC 3′) and the reverse primer (5′ GTGCAGAACCTGCG**GTC**TGACCACCACCG 3′) were used to make the E216Q enzyme. The forward primer (5′ CATCACCTGCAGGGT**GCG**GTGACCCGCATC 3′) and the reverse primer (5′ GATGCGGGTCAC**CGC**ACCCTGCAGGTGATG 3′) were used to make the R301A enzyme. The forward primer (5′ GTGTTATCTCCCCG**ATG**GCCACCATTTATACG 3′) and the reverse primer (5′

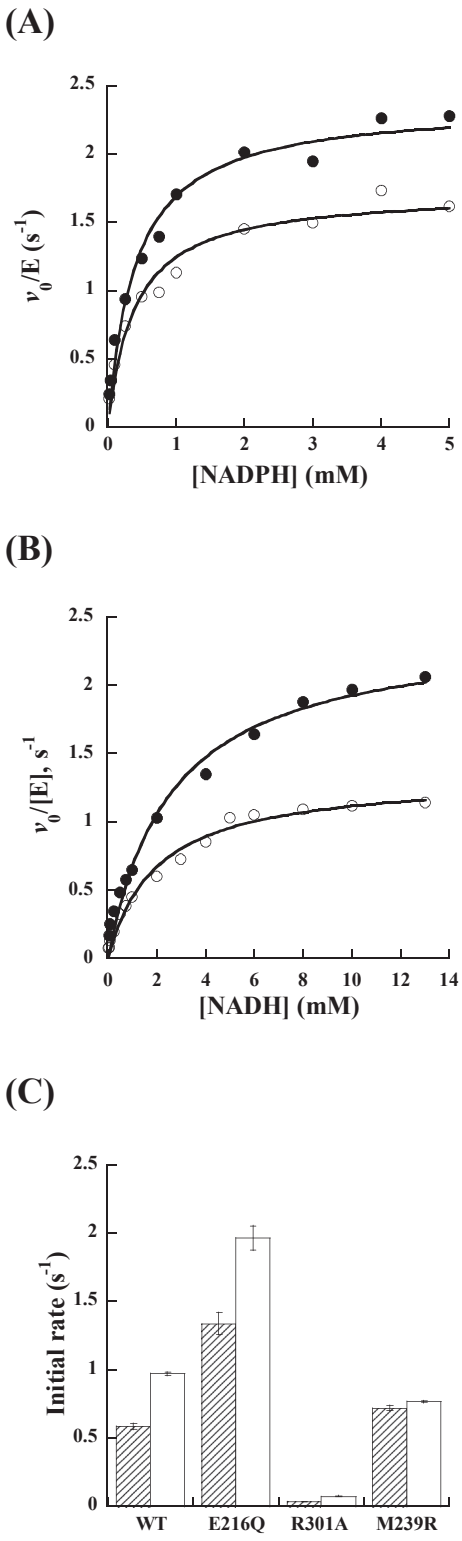

Fig. 4. Steady-state oxygen consumption for E216Q. (A) E216Q oxygen consumption rates as a function of NADPH without L-Lys (○) or with 2 mM L-Lys (●), and (B) rates as a function of NADH without L-Lys (○) or with 2 mM L-Lys (●). (C) Relative oxygen consumption activity of mutant proteins *vs.* wtNbtG at 2 mM NADPH in the absence (-, plain) or presence of (+, shaded) 2 mM L-Lys.

Table 1
Steady-state kinetics parameters determined by measuring oxygen consumption.

	$k_{cat,}$ (s^{-1})	$K_{m,}$ (mM)	$k_{cat}/K_{m,}$ (M^{-1} s^{-1})	$k_{cat,}$ (s^{-1})	$K_{m,}$ (mM)	$k_{cat}/K_{m,}$ (M^{-1} s^{-1})
NADPH	No L-Lys			2 mM L-Lys		
wtNbtG[a]	0.58 ± 0.02	0.2 ± 0.02	2900 ± 300	1.08 ± 0.01	0.14 ± 0.01	7700 ± 500
E216Q	1.7 ± 0.08	0.38 ± 0.07	4500 ± 715	2.4 ± 0.09	0.40 ± 0.06	5950 ± 700
R301A	ND	ND	ND	ND	ND	26 ± 2.7
M239R	–	–	–	0.98 ± 0.02	0.09 ± 0.006	10700 ± 730
NADH	No L-Lys			2 mM L-Lys		
wtNbtG[a]	0.32 ± 0.01	0.36 ± 0.05	900 ± 100	1.29 ± 0.04	0.40 ± 0.04	3300 ± 400
E216Q	1.3 ± 0.05	2.0 ± 0.25	670 ± 60	2.4 ± 0.1	2.6 ± 0.4	940 ± 100
R301A	0.54 ± 0.05	2.1 ± 0.5	255 ± 40	0.8 ± 0.05	1.5 ± 0.3	545 ± 70
M239R	–	–	–	0.7 ± 0.02	0.08 ± 0.01	8900 ± 1100

Conditions: the experiment was performed at 25 °C in 100 mM sodium phosphate buffer, pH 7.5. ND: Not Detected.
[a] Values from Binda et al., 2015 [12].

CGTATAAATGGTGGC**CAT**CGGGGAGATAACAC 3′) were used to make the M239R enzyme. Codons of mutated positions are underlined and bolded.

2.3. Protein expression and purification

All NbtG mutant proteins were expressed in *E. coli* BL21(DE3)-T^{1R} cells and purified as previously described for wtNbtG [12]. The recombinant proteins were overexpressed as 8xHis-MBP fusion proteins. In general, 3 L of terrific broth (TB) supplemented with 25 μg/mL of kanamycin were grown [27]. Purification was done following standard procedures previously reported for wtNbtG [12]. The 8xHis-MBP fusions were cleaved after the purification step with a nickel immobilized affinity chromatography (IMAC) column [12].

2.4. Determination of flavin extinction coefficient and incorporation

For all three mutant proteins, extinction coefficients were determined based on the extinction coefficient of free FAD (11.3 mM^{-1} cm^{-1} at 450 nm), following previously published procedures [12,28]. FAD incorporation was determined by comparing the protein concentration measured using the Bradford assay (BioRad) to the concentration measured based on the flavin spectrum.

2.5. Oxygen consumption assay

The initial reaction velocity was calculated by measuring oxygen consumption in 1 mL of 100 mM sodium phosphate buffer, pH 7.5. The reaction was initiated with 1 μM mutant enzyme and monitored using a Hansatech Oxygraph Plus System (Norfolk, England) at 25 °C with constant stirring. For E216Q, the activity at various concentrations of NADPH (0.025–5 mM), NADH (0.025–13 mM), or L-Lys (0–10 mM) were determined. When L-Lys was varied, assays were saturated with either 2 mM NADPH or 10 mM NADH. L-Lys was kept constant at 2 mM when NAD(P)H was varied. The activity of R301A was determined with NADPH (0.025–20 mM) or NADH (0.025–6 mM) at a constant concentration of L-Lys (2 mM). The activity of R301A at varying concentrations of L-Lys (0.025–5 mM) was determined at a constant NADH concentration of 8 mM. For M239R, NADPH was varied between 0.1 and 5 mM, while L-Lys was kept constant at 2 mM.

2.6. Product formation assay

The formation of N^6-hydroxy-L-Lys was measured using a variation of the Casky iodine oxidation assay [29,30]. Briefly, each reaction consisted of 104 μL of 100 mM sodium phosphate buffer (pH 7.5) and varying concentrations of L-Lys or NAD(P)H with a constant concentration of the other substrate. For E216Q, when NADPH (0.025–10 mM) was varied, L-Lys was constant at 30 mM. The activity, as a function of L-Lys concentration (1–100 mM), was measured at 2 mM NADPH. For R301A, similar experiments were performed with varying NADH concentrations (0.025–10 mM) at constant L-Lys concentration (2 mM). When L-Lys was varied (0.025–10 mM), NADH was kept constant at 2 mM. For M239R, NADPH was varied between (0.025–2 mM) with a constant 2 mM L-Lys. Reactions were initiated by the addition of 1 μM E216Q, M239R, or 2 μM R301A, and the reaction was allowed to proceed for 5 min (E216Q) or 10 min (R301A, M239R) at 25 °C with shaking at 750 rpm. All samples were run in triplicate.

2.7. Flavin reduction

These experiments were carried out using an SX-20 stopped-flow spectrophotometer (Applied Photophysics, Leatherhead, UK) in an anaerobic glove box (Coy, Grass Lake, MI) at 25 °C in 100 mM sodium phosphate buffer, pH 7.5. Buffer solutions and enzyme stocks were made anaerobic as described previously [31]. The rate of flavin reduction was monitored after mixing oxidized E216Q or R301A (15 μM, after mixing) with an equal volume of various concentrations of NAD(P)H (0.025–5 mM after mixing for E216Q or 0.1–8 mM for R301A). Flavin spectra changes at 450 nm were monitored on a logarithmic time scale until full flavin reduction was observed. Data were fit to a three or two-phase exponential decay equation (Eqs. (1) and (2)). In these equations, A is the change in absorbance, k_{obs} is the observed rate for each phase, C is the final absorbance, t is the time.

To obtain the maximum rate constant of flavin reduction (k_{red}) and the K_D value, the observed rates (k_{obs}) as a function of NAD(P)H concentration were analyzed using equation (3) (Eq. (3)) [32].

$$v = C + A_1 e^{-(kobs_1 t)} + A_2 e^{-(kobs_2 t)} + A_3 e^{-(kobs_3 t)} \quad (1)$$

$$v = C + A_1 e^{-(kobs_1 t)} + A_2 e^{-(kobs_2 t)} \quad (2)$$

$$k_{obs} = \frac{k_{red} \times [NAD(P)H]}{K_D + [NAD(P)H]} \quad (3)$$

3. Results

3.1. Purification of mutant proteins

Overall yields of ~35, 150, and 36 mg were obtained from 50 g cells of E216Q, R301A, and M239R, respectively. The purified

proteins were stored in 100 mM sodium phosphate buffer, 50 mM NaCl, pH 7.5, at −80 °C at a concentration of ~200 μM (based on the flavin content) in 30 μL aliquots.

3.2. Determination of flavin extinction coefficient and incorporation

The flavin spectra recorded for the mutant proteins were similar to that of wtNbtG. Extinction coefficients at 450 nm were almost identical with values of 12.8 $mM^{-1}cm^{-1}$ for E216Q and 12.6 $mM^{-1}cm^{-1}$ for both R301A and M239R compared to 12.6 $mM^{-1}cm^{-1}$ for wtNbtG [12]. Non-covalently bound FAD incorporation was ~77% and 76% for R301A and M239R, respectively, but slightly increased to 83% in E216Q compared to 75% in the wtNbtG.

3.3. Oxygen consumption assay

The initial rates of oxygen consumption were measured to determine the kinetic parameters of the NbtG mutant enzymes. Compared to wtNbtG, in the absence of L-Lys and using NADPH as the coenzyme, E216Q showed a ~ 3-fold higher k_{cat} value with only a 2-fold increase in the K_m value. Catalytic efficiency increased only 1.5-fold due to the increase in the k_{cat} and K_m (Fig. 4 and Table 1). Addition of 2 mM L-Lys increased the k_{cat} value for E216Q similarly to wtNbtG behavior in the presence of L-Lys, while the K_m value for NADPH was increased ~ 2-fold for E216Q (Table 1, Fig. 4). R301A was almost inactive in the absence or presence of L-Lys with up to 20 mM NADPH. Because of the low activity and high apparent K_m value, only the k_{cat}/K_m value could be calculated and it was ~300-fold lower than for wtNbtG (Table 1, Fig. 5). The kinetic parameters of M239R with NADPH in the presence of L-Lys were not significantly different than those of wtNbtG. However, using NADH, the k_{cat} and K_m values decreased by 2 and 5-fold, respectively. These changes produced a ~3-fold increase in the k_{cat}/K_m value (Table 1).

Using NADH in the absence of L-Lys, the k_{cat} value increased ~4-fold and ~2-fold for E216Q and R301A, respectively, with an ~6-fold increase in the K_m value for both mutant enzymes. The k_{cat}/K_m value was similar to wtNbtG for E216Q but decreased ~4-fold for R301A due to the increase in the K_m value. The presence of L-Lys leads to a ~2-fold increase in the k_{cat} values for R301A and E216Q, while the K_m values did not change in the presence of L-Lys. k_{cat}/K_m values were ~ 6-fold lower than for wtNbtG for both mutant proteins because of high K_m values (Figs. 4 and 5).

For wtNbtG and R301A, the initial rates increased as a function of L-Lys concentration, with substrate inhibition observed at high levels (Fig. 5). For E216Q, there was no such L-Lys concentration dependence (~1 s^{-1} at all concentrations tested - data not shown).

For general comparison, the activity of the mutant enzymes at 2 mM NADPH in the absence or presence of 2 mM L-Lys was measured and the initial velocities were compared with wtNbtG. R301A showed almost no activity, while E216Q exhibited higher oxidase activity. The presence of L-Lys enhanced the rates for only E216Q and wtNbtG by 30% and 38%, respectively. However, M239R had similar kinetic parameters with NADPH as wtNbtG (Fig. 4c).

3.4. Product formation assay

Activity of NbtG variants was also determined by measuring the initial rates of hydroxylated L-Lys production (Table 2). E216Q showed a ~2-fold higher k_{cat} and k_{cat}/K_m with similar K_m and K_I values for NADPH. When varying L-Lys, the K_m and K_I values were increased ~30-fold and 4-fold, respectively, which in turn, decreased the catalytic efficiency by 10-fold (Fig. 6). In contrast, no product was detected for R301A with 2 mM L-Lys and various

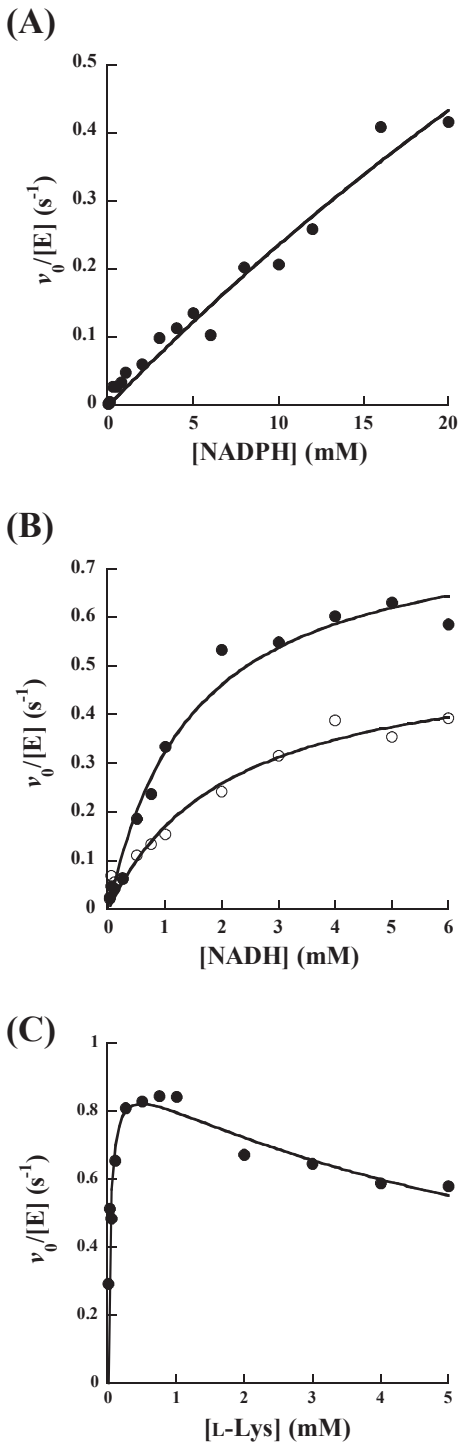

Fig. 5. Steady-state oxygen consumption for R301A. (A) As a function of NADPH (saturated with 2 mM L-Lys). (B) As a function of NADH without L-Lys (○) or with 2 mM L-lysine (●). (C) As a function of L-Lys (saturated with 8 mM NADH).

NADPH concentrations up to 20 mM (data not shown). However, using NADH allowed the reaction to proceed with ~2-fold lower k_{cat} and 4-fold higher K_m values, which resulted in an 8-fold lower k_{cat}/K_m value (Table 2). In addition, varying L-Lys resulted in no significant changes in any of the kinetic parameters (Fig. 7). For M239R, varying NADPH led to the decrease of k_{cat}, K_m, and k_{cat}/K_m by ~24, 9, and 3-fold, respectively, and an increase in the inhibition constant of only 2-fold (Table 2).

Table 2
NbtG steady-state kinetic parameters for hydroxylated L-Lys formation.

	wtNbtG[a]	E216Q	M239R	wtNbtG[a]	R301A
	NADPH			NADH	
k_{cat} (s^{-1})	0.32 ± 0.02	0.62 ± 0.07	0.013 ± 0.0007	0.62 ± 0.08	0.28 ± 0.01
$K_{m,\ NAD(P)H}$ (mM)	0.7 ± 0.2	0.9 ± 0.2	0.08 ± 0.03	0.6 ± 0.1	2.1 ± 0.3
$k_{cat}/K_{m,\ NAD(P)H}$ ($M^{-1}s^{-1}$)	460 ± 130	700 ± 170	160 ± 60	1100 ± 300	130 ± 20
$K_{I,\ NAD(P)H}$ (mM)	2.4 ± 0.6	4 ± 1	5.0 ± 2.0	5.7 ± 1.7	14 ± 4
	2 mM NADPH			2 mM NADH	
$K_{m,\ L\text{-}Lys}$ (mM)	0.35 ± 0.05	11 ± 2	–	0.9 ± 0.3	0.5 ± 0.1
$k_{cat}/K_{m,\ L\text{-}Lys}$ ($M^{-1}s^{-1}$)	910 ± 140	90 ± 20	–	580 ± 230	540 ± 190
$K_{I,\ L\text{-}Lys}$ (mM)	15 ± 3	60 ± 10	–	6.3 ± 2.5	7.5 ± 2.0
% Uncoupling	70	75	98	52	65

Conditions: the experiment was performed at 25 °C in 100 mM sodium phosphate buffer, pH 7.5. For the E216Q and R301A reactions that varied NAD(P)H, L-Lys was kept constant at 30 and 2 mM, respectively.
[a] Values from Binda et al., 2015 [12].

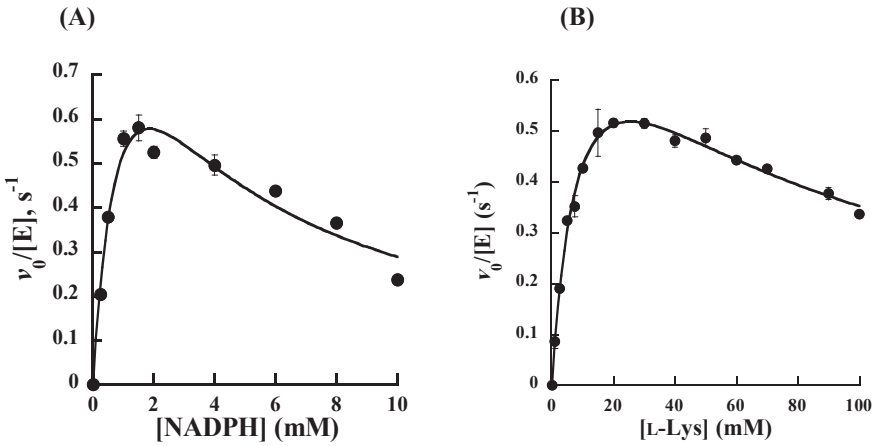

Fig. 6. Steady-state L-Lys hydroxylation for E216Q. (A) As a function of NADPH (saturated with 30 mM L-Lys). (B) As a function of L-Lys (saturated with 2 mM NADPH).

3.5. Flavin reduction

The reaction of oxidized E216Q or R301A was monitored at 450 nm as a function of NADPH concentration to determine the rate constant for flavin reduction (k_{red}) (Fig. 8). E216Q reduction showed three kinetic phases instead of the two observed in wtNbtG (Table 3 and Fig. 8). For wtNbtG, it was speculated that the multiple phases were originated by the presence of multiple enzyme forms (some less active) [12]. It is possible that multiple enzyme forms are present the samples of E216Q. Analysis of the first phase permitted the calculation of k_{red} and K_D values that were 6-fold higher than for wtNbtG. The second phase showed kinetic parameters that were very similar to those calculated for the first phase observed in wtNbtG. Finally, the third phase had the same reduction rate

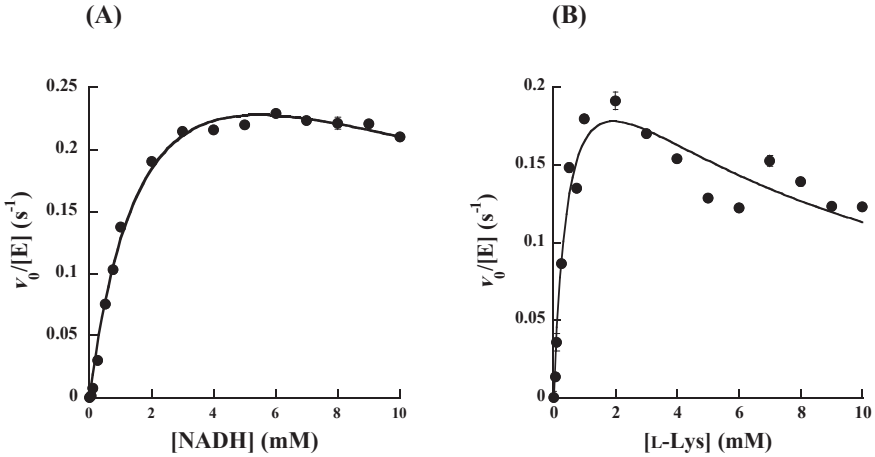

Fig. 7. Steady-state L-Lys hydroxylation for R301A. (A) As a function of NADH (saturated with 2 mM L-Lys). (B) As a function of L-Lys (saturated with 2 mM NADH).

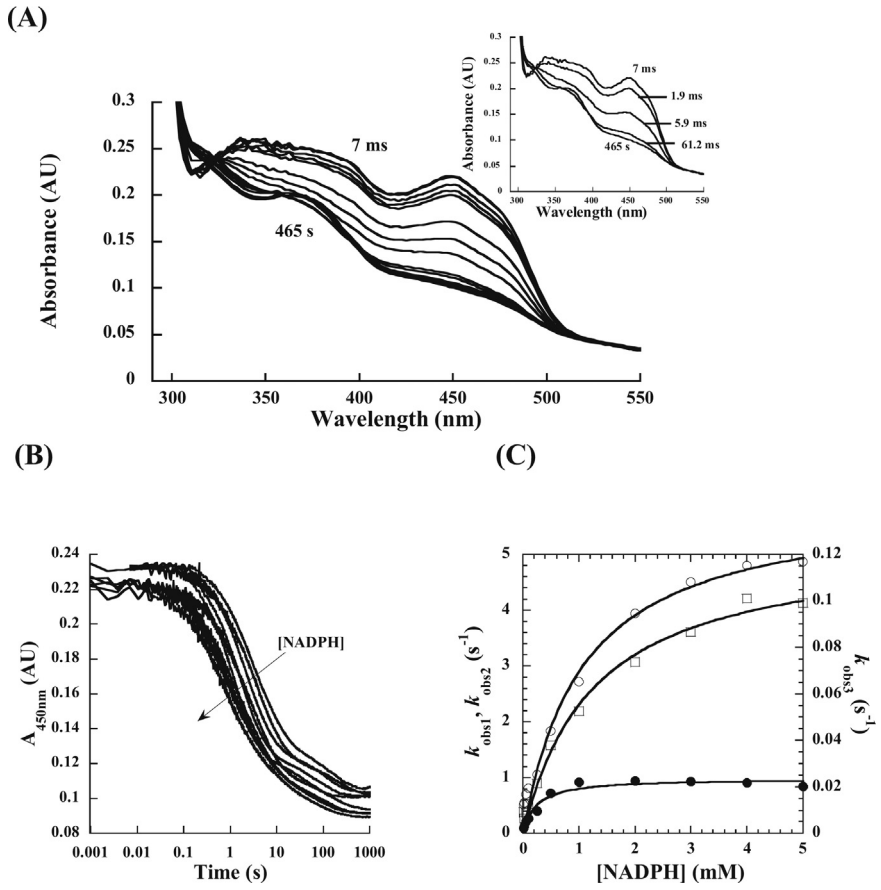

Fig. 8. E216Q reduction with NADPH. (A) Spectral changes for 15 μM E216Q with 15 μM NADPH, the inset shows different time traces. (B) Changes in the flavin absorbance at 450 nm at various concentrations of NADPH (0.025–5 mM) in the absence of L-Lys. (C) Dependence of the k_{obs} values as a function of NADPH during the first (○), second (●), and third (□) phases. All data were fit to the triple exponential decay equation.

observed in the second phase of wtNbtG, but the K_D showed a ~6-fold higher value [12]. Reduction of R301A was very slow, with complete reduction observed at ≥ 8 mM NADPH with a $k_{red(app)}$ value of 0.09 s^{-1} and 0.003 s^{-1} for the first and second phase, respectively.

4. Discussion

Flavin-dependent monooxygenases have been classified into eight groups (A-H) based on their structural and functional properties [33]. These enzymes catalyze hydroxylation, sulfoxidation, epoxidation, Baeyer–Villiger oxidation, and halogenation reactions through the incorporation of a single oxygen atom into a variety of substrates [34,35]. They have received great attention in environmental, industrial, and pharmaceutical applications due to their regio- and enantioselective catalytic activity and their wide-spectrum of substrate reactivity [36–38].

NMOs are members of the class B flavin monooxygenases and catalyze the hydroxylation of the side chain amine of L-Lys or L-Orn. The hydroxylamine product makes up the iron-binding site in hydroxamate-containing siderophores [6,33,34]. Biosynthesis of siderophores is one of the virulence mechanisms adopted by many pathogens such as *Pseudomonas aeruginosa, Nocardia* sp., *Mycobacteria* sp., as well as fungi such as *Aspergillus fumigatus* [39,40].

Members of class B flavin monooxygenases utilize NADPH and/or NADH as their redox partners. Despite the minor structural difference of one phosphate group between the two coenzymes, members of this class are highly selective for NADPH over NADH with few exceptions. For example, phenylacetone monooxygenase (PAMO) and PvdA are strictly selective for NADPH [41,42], while cyclohexanone monooxygenase (CHMO) and 4-hydroxyacetophenone monooxygenase (HAPMO) are less strict, displaying an ~ 600–700-fold preference for NADPH over NADH [43]. Lower selectivity has been reported of 20-fold NADPH preference in SidA [13]. This ratio decreased to an ~ 2-fold NADPH preference in NbtG, and shifted towards NADH preference in L-Lys ^{6}*N*-hydroxylase from *Mycobacterium smegmatis* (MbsG) and

Table 3
Pre-steady state kinetic parameters with NAD(P)H in the absence of L-Lys.

	wtNbtG[a]	E216Q
	NADPH	
First phase		
$k_{red,\ NADPH}$ (s^{-1})	1.00 ± 0.03	6.0 ± 0.4
$K_{D,\ NADPH}$ (mM)	0.20 ± 0.03	1.1 ± 0.2
$k_{red}/K_{D,\ NADPH}$ ($M^{-1}\ s^{-1}$)	5000 ± 760	5650 ± 800
Second phase		
$k_{red,\ NADPH}$ (s^{-1})	0.12 ± 0.002	1.00 ± 0.05
$K_{D,\ NADPH}$ (mM)	0.23 ± 0.03	0.23 ± 0.05
$k_{red}/K_{D,\ NADPH}$ ($M^{-1}\ s^{-1}$)	520 ± 70	4300 ± 800
Third phase		
$k_{cat,\ L\text{-}lys}$ (s^{-1})	ND	0.13 ± 0.007
$K_{m,\ L\text{-}lys}$ (mM)	ND	1.3 ± 0.2
$k_{cat}/K_{m,\ L\text{-}lys}$ ($M^{-1}\ s^{-1}$)	ND	100 ± 10

Conditions: the experiment was performed at 25 °C in 100 mM sodium phosphate buffer, pH 7.5. ND: Not detected.
[a] Values from Binda et al., 2015 [12].

flavoprotein monooxygenase (FPMO) from *Stenotrophomonas maltophilia* with an ~ 3 and 1.5-fold over NADPH, respectively [12,30,44].

The NMOs SidA and PvdA have been structurally and biochemically characterized. They share similar mechanistic and structural features, such as high NADPH and L-Orn selectivity [13,19,23]. Furthermore, they efficiently catalyze highly coupled reactions with low amount of oxygen reactive species (by-product) formation. These enzymes stabilize the C4a-hydroperoxyflavin *via* interactions mediated by $NADP^+$, which remains bound after FAD reduction to ensure efficient substrate hydroxylation [15,16,18,21]. In contrast, NbtG catalyzes the hydroxylation of L-Lys as well as D-Lys, utilizes both NADPH and NADH, and does not stabilize C4a-hydroperoxyflavin. Thus, the reaction results in the production of significant amounts of hydrogen peroxide and superoxide (i.e., a highly uncoupled reaction) [12]. Interestingly, similar results have been reported previously for MbsG, which has 53% identity to NbtG [45]. Unfortunately, there is no current structural information that could aid in the interpretation of the mechanistic differences between SidA, PvdA, and NbtG as there are no structures either with bound $NADP^+$ or L-Lys.

However, based on sequence alignment of NbtG and other mycobacteria-related species, as well as structure superimposition with SidA and PvdA (Figs. 1–3), P238, M239, and R301 were proposed as residues that could interact with the 2′ -phosphate of NADPH, as potential counterparts for the Arg residue found in SidA (R279) and PvdA (R240), which is responsible for coenzyme selectivity [16,18].

Indeed, P238 orientation shows clashes with the NADP(H) molecule bound in the SidA crystal (Fig. 2). However, we previously reported an NADPH domain rotation in NbtG that could lead to different binding of NADPH. It was previously shown that P238R shifted coenzyme selectivity exclusively to NADPH, but, the reaction rate was compromised with no actual improvement on the reaction coupling [12]. Within the same flexible loop containing P238, the neighboring residue M239 was replaced by Arg. The biochemical characterization of M239R showed that it was active with both NADPH and NADH. Replacement of M239 to Arg did not change the oxygen consumption k_{cat} or K_{NADPH} values, but it decreased the K_{NADH} value ~ 5-fold compared to wtNbtG. However, the product formation rate drastically decreased giving rise to a 40% increase in reaction uncoupling. This data does not indicate that the addition of a positive charge at position 239 improves NbtG's selectivity and monooxygenase activity. Further structural analysis showed that the R301 in NbtG was highly conserved among related *Mycobacteria* L-Lys hydroxylases (Figs. 1 and 3). The R301 residue lies within a different loop in the NADPH binding domain and could possibly orient close to the 2′ -phosphate of the adenine-ribose moiety. Steady-state kinetic results of R301A showed a drastic decrease in activity with NADPH but not with NADH. Additionally, complete FAD reduction could not be observed at NADPH concentrations lower than 8 mM. Similar replacement of R279 to Ala or Glu in SidA affected only the $K_{D,NADPH}$ value ~270 and 1600-fold, respectively (16). Clearly, the results suggest that R301 plays a major role in NADPH binding and might interact with the 2′ -phosphate moiety of NDA(P)H.

Next, to test if E216 plays a role in catalysis, we studied the kinetics of NbtG E216Q. Steady-state kinetic analysis revealed an increase in k_{cat} values of oxygen consumption as well as product formation with no significant effect on coenzyme binding. However, the $K_{m,L\text{-}Lys}$ value increased ~30-fold, implying a potential role in L-Lys binding. This data is supported by the potential H-bonding observed between the N^6-atom of L-Lys and the side chain carboxyl of Glu216 (Fig. 3). Interestingly, this interaction is not predicted for the equivalent residue in SidA (Gln256) as the distance to either of the L-Orn or L-Lys side chain amino groups is not optimal for such interactions. In NbtG, E216 might be able to interact with L-Lys because of the displacement of the α-helix caused by NADPH binding domain rotation [12,26].

Furthermore, the appearance of a new, faster phase of reduction upon NADPH binding accompanied by changes in FAD spectra could be attributed to the unstable binding of NADPH (resulting in the higher K_D value) due to removal of the negative charge of Glu216. This might lead to changes in the FAD microenvironment after hydride transfer (Fig. 8a). Substitution of N323 to Ala in SidA significantly increased the flavin reduction rate by ~20-fold. In addition, steady-state kinetics have shown that substrate binding ($K_{m(L\text{-}Orn)}$) was increased ~ 15-fold with no observed effect on NADPH binding. Thus, N323 was proposed to hydrogen bond with the nicotinamide ribose of NADPH as well as contribute to L-Orn binding to balance flavin reduction and substrate binding [14]. In Sida, the interaction of N323 with NADPH was proposed to regulate the position of $NADP^+$, which is believe to require significant movement [22]. It is possible that in NbtG E216 is involved in L-Lys binding and in the modulation of NAD(H) interaction during reduction.

Our results show that sequence alignment alone is not sufficient to assign amino acid functionality, as different conformational characteristics should be considered. The data described here is consistent with R301 playing a role in NADPH selectivity in NbtG. In addition, E216 plays a role in L-Lys binding and FAD reduction in NbtG.

Acknowledgements

This work was supported in part by a grant from the National Science Foundation MCB 1021384. H. A. was supported by a Joint Supervision Fellowship from the Cultural Affairs and Missions sector of the Egyptian Ministry of Higher Education.

References

[1] Y.K. Kim, H. Sung, J. Jung, S.N. Yu, J.Y. Lee, S.H. Kim, S.H. Choi, Y.S. Kim, J.H. Woo, S.O. Lee, Y.P. Chong, Impact of immune status on the clinical characteristics and treatment outcomes of nocardiosis, Diagn. Microbiol. Infect. Dis. 85 (4) (2016) 482–487.
[2] P.I. Lerner, Nocardiosis, Clin. Infect. Dis. 22 (6) (1996) 891–903.
[3] R. Schlaberg, R.C. Huard, P. Della-Latta, Nocardia cyriacigeorgica, an emerging pathogen in the United States, J. Clin. Microbiol. 46 (1) (2008) 265–273.
[4] J.W. Wilson, Nocardiosis: updates and clinical overview, Mayo Clin. Proc. 87 (4) (2012) 403–407.
[5] T.C. Sorrell, D.H. Mitchell, J.R. Iredell, S.C.A. Chen, Nocardia species, in: J.E. Bennett, R. Dolin, M.J. Blaser (Eds.), Principles and Practice of Infectious Diseases, eighth ed., Elsevier Churchill Livingstone, Philadelphia, PA, 2015, pp. 2853–2863.
[6] Y. Hoshino, K. Chiba, K. Ishino, T. Fukai, Y. Igarashi, K. Yazawa, Y. Mikami, J. Ishikawa, Identification of nocobactin NA biosynthetic gene clusters in Nocardia farcinica, J. Bacteriol. 193 (2) (2011) 441–448.
[7] J. Ishikawa, A. Yamashita, Y. Mikami, Y. Hoshino, H. Kurita, K. Hotta, T. Shiba, M. Hattori, The complete genomic sequence of Nocardia farcinica IFM 10152, Proc. Natl. Acad. Sci. U. S. A 101 (41) (2004) 14925–14930.
[8] J.B. Neilands, Siderophores: structure and function of microbial iron transport compounds, J. Biol. Chem. 270 (45) (1995) 26723–26726.
[9] A. Szebeszczyk, E. Olshvang, A. Shanzer, P.L. Carver, E. Gumienna-Kontecka, Harnessing the power of fungal siderophores for the imaging and treatment of human diseases, Coord. Chem. Rev. (2016) [in press].
[10] R.J. Abergel, M.K. Wilson, J.E. Arceneaux, T.M. Hoette, R.K. Strong, B.R. Byers, K.N. Raymond, Anthrax pathogen evades the mammalian immune system through stealth siderophore production, Proc. Natl. Acad. Sci. U. S. A 103 (49) (2006) 18499–18503.
[11] Y. Hoshino, K. Chiba, K. Ishino, T. Fukai, Y. Igarashi, K. Yazawa, Y. Mikami, J. Ishikawa, Identification of nocobactin NA biosynthetic gene clusters in Nocardia farcinica, J. Bacteriol. 193 (2) (2011) 441–448.
[12] C. Binda, R.M. Robinson, J.S. Martin Del Campo, N.D. Keul, P.J. Rodriguez, H.H. Robinson, A. Mattevi, P. Sobrado, An unprecedented NADPH domain conformation in lysine monooxygenase NbtG provides insights into uncoupling of oxygen consumption from substrate hydroxylation, J. Biol. Chem. 290 (20) (2015) 12676–12688.

[13] S.W. Chocklett, P. Sobrado, Aspergillus fumigatus SidA is a highly specific ornithine hydroxylase with bound flavin cofactor, Biochemistry 49 (31) (2010) 6777–6783.
[14] R. Robinson, I.A. Qureshi, C.A. Klancher, P.J. Rodriguez, J.J. Tanner, P. Sobrado, Contribution to catalysis of ornithine binding residues in ornithine N5-monooxygenase, Arch. Biochem. Biophys. 585 (2015) 25–31.
[15] J. Olucha, A.L. Lamb, Mechanistic and structural studies of the N-hydroxylating flavoprotein monooxygenases, Bioorg. Chem. 39 (5–6) (2011) 171–177.
[16] R. Robinson, S. Franceschini, M. Fedkenheuer, P.J. Rodriguez, J. Ellerbrock, E. Romero, M.P. Echandi, J.S. Martin Del Campo, P. Sobrado, Arg279 is the key regulator of coenzyme selectivity in the flavin-dependent ornithine monooxygenase SidA, Biochim. Biophys. Acta 1844 (4) (2014) 778–784.
[17] R. Robinson, S. Badieyan, P. Sobrado, C4a-hydroperoxyflavin formation in N-hydroxylating flavin monooxygenases is mediated by the 2'-OH of the nicotinamide ribose of NADP(+), Biochemistry 52 (51) (2013) 9089–9091.
[18] J. Olucha, K.M. Meneely, A.S. Chilton, A.L. Lamb, Two structures of an N-hydroxylating flavoprotein monooxygenase: ornithine hydroxylase from Pseudomonas aeruginosa, J. Biol. Chem. 286 (36) (2011) 31789–31798.
[19] H.-J. Plattner, P. Pfefferle, A. Romaguera, S. Waschiitza, H. Diekmann, Isolation and some properties of lysineN 6-hydroxylase fromEscherichia coli strain EN222, Biol. Met. 2 (1) (1989) 1–5.
[20] K.M. Meneely, A.L. Lamb, Biochemical characterization of a flavin adenine dinculeotide-dependent monooxygenase, ornithine hydroxylase from Pseudomonas aeruginosa, suggests a novel reaction mechanism, Biochemistry 46 (42) (2007) 11930–11937.
[21] E. Romero, M. Fedkenheuer, S.W. Chocklett, J. Qi, M. Oppenheimer, P. Sobrado, Dual role of NADP(H) in the reaction of a flavin dependent N-hydroxylating monooxygenase, Biochim. Biophys. Acta 1824 (6) (2012) 850–857.
[22] C. Shirey, S. Badieyan, P. Sobrado, Role of Ser-257 in the sliding mechanism of NADP(H) in the reaction catalyzed by the Aspergillus fumigatus flavin-dependent ornithine N5-monooxygenase SidA, J. Biol. Chem. 288 (45) (2013) 32440–32448.
[23] K.M. Meneely, E.W. Barr, J.M. Bollinger Jr., A.L. Lamb, Kinetic mechanism of ornithine hydroxylase (PvdA) from Pseudomonas aeruginosa: substrate triggering of O2 addition but not flavin reduction, Biochemistry 48 (20) (2009) 4371–4376.
[24] J.A. Mayfield, R.E. Frederick, B.R. Streit, T.A. Wencewicz, D.P. Ballou, J.L. DuBois, Comprehensive spectroscopic, steady state, and transient kinetic studies of a representative siderophore-associated flavin monooxygenase, J. Biol. Chem. 285 (40) (2010) 30375–30388.
[25] M. Stehr, H. Diekmann, L. Smau, O. Seth, S. Ghisla, M. Singh, P. Macheroux, A hydrophobic sequence motif common to N-hydroxylating enzymes, Trends biochem. Sci. 23 (2) (1998) 56–57.
[26] S. Franceschini, M. Fedkenheuer, N.J. Vogelaar, H.H. Robinson, P. Sobrado, A. Mattevi, Structural insight into the mechanism of oxygen activation and substrate selectivity of flavin-dependent N-hydroxylating monooxygenases, Biochemistry 51 (36) (2012) 7043–7045.
[27] B.G. Fox, P.G. Blommel, Autoinduction of protein expression, Curr. Protoc. Protein. Sci. (2009). Chapter 5:Unit 5.23.
[28] P. Macheroux, Uv-visible spectroscopy as a tool to study flavoproteins, in: S.K. Chapman, G.A. Reid (Eds.), Flavoprotein Protocols, Humana Press, Totowa, NJ, 1999, pp. 1–7.
[29] T. Csaky, On the estimation of bound hydroxylamine in biological materials, Acta Chem. Scand. 2 (5–6) (1948) 450–454.
[30] R. Robinson, P. Sobrado, Substrate binding modulates the activity of Mycobacterium smegmatis G, a flavin-dependent monooxygenase involved in the biosynthesis of hydroxamate-containing siderophores, Biochemistry 50 (39) (2011) 8489–8496.
[31] E. Romero, R. Robinson, P. Sobrado, Monitoring the reductive and oxidative half-reactions of a flavin-dependent monooxygenase using stopped-flow spectrophotometry, J. Vis. Exp. (61) (2012).
[32] S. Strickland, G. Palmer, V. Massey, Determination of dissociation constants and specific rate constants of enzyme-substrate (or protein-ligand) interactions from rapid reaction kinetic data, J. Biol. Chem. 250 (11) (1975) 4048–4052.
[33] M.M. Huijbers, S. Montersino, A.H. Westphal, D. Tischler, W.J. van Berkel, Flavin dependent monooxygenases, Arch. Biochem. Biophys. 544 (2014) 2–17.
[34] W.J. van Berkel, N.M. Kamerbeek, M.W. Fraaije, Flavoprotein monooxygenases, a diverse class of oxidative biocatalysts, J. Biotechnol. 124 (4) (2006) 670–689.
[35] V. Massey, Activation of molecular oxygen by flavins and flavoproteins, J. Biol. Chem. 269 (36) (1994) 22459–22462.
[36] Y. Tao, A. Fishman, W.E. Bentley, T.K. Wood, Oxidation of benzene to phenol, catechol, and 1,2,3-trihydroxybenzene by toluene 4-monooxygenase of Pseudomonas mendocina KR1 and toluene 3-monooxygenase of Ralstonia pickettii PKO1, Appl. Environ. Microbiol. 70 (7) (2004) 3814–3820.
[37] M. Shimizu, A. Shiraishi, A. Sato, S. Nagashima, H. Yamazaki, Potential for drug interactions mediated by polymorphic flavin-containing monooxygenase 3 in human livers, Drug Metab. Pharmacokinet. 30 (1) (2015) 70–74.
[38] M.J. Fink, M.D. Mihovilovic, Non-hazardous Baeyer-Villiger oxidation of levulinic acid derivatives: alternative renewable access to 3-hydroxypropionates, Chem. Commun. (Camb.) 51 (14) (2015) 2874–2877.
[39] A.H. Hissen, A.N. Wan, M.L. Warwas, L.J. Pinto, M.M. Moore, The Aspergillus fumigatus siderophore biosynthetic gene sidA, encoding L-ornithine N5-oxygenase, is required for virulence, Infect. Immun. 73 (9) (2005) 5493–5503.
[40] M. Miethke, M.A. Marahiel, Siderophore-based iron acquisition and pathogen control, Microbiol. Mol. Biol. Rev. 71 (3) (2007) 413–451.
[41] L. Ge, S.Y. Seah, Heterologous expression, purification, and characterization of an L-ornithine N5-hydroxylase involved in pyoverdine siderophore biosynthesis in Pseudomonas aeruginosa, J. Bacteriol. 188 (20) (2006) 7205–7210.
[42] M.W. Fraaije, J. Wu, D.P. Heuts, E.W. van Hellemond, J.H. Spelberg, D.B. Janssen, Discovery of a thermostable Baeyer-Villiger monooxygenase by genome mining, Appl. Microbiol. Biotechnol. 66 (4) (2005) 393–400.
[43] N.M. Kamerbeek, M.W. Fraaije, D.B. Janssen, Identifying determinants of NADPH specificity in Baeyer-Villiger monooxygenases, Eur. J. Biochem. 271 (11) (2004) 2107–2116.
[44] C.N. Jensen, S.T. Ali, M.J. Allen, G. Grogan, Mutations of an NAD (P) H-dependent flavoprotein monooxygenase that influence cofactor promiscuity and enantioselectivity, FEBS Open Bio 3 (2013) 473–478.
[45] R.M. Robinson, P.J. Rodriguez, P. Sobrado, Mechanistic studies on the flavin-dependent N(6)-lysine monooxygenase MbsG reveal an unusual control for catalysis, Arch. Biochem. Biophys. 550–551 (2014) 58–66.
[46] P. Di Tommaso, S. Moretti, I. Xenarios, M. Orobitg, A. Montanyola, J.-M. Chang, J.-F. Taly, C. Notredame, T-Coffee: a web server for the multiple sequence alignment of protein and RNA sequences using structural information and homology extension, Nucleic Acids Res. 39 (suppl 2) (2011) W13–W17.